FULL PAPER

Analysis of a Compound Class with Triplet States Stabilized by Potentially Baird-Aromatic [10]Annulenyl Dicationic Rings

Kjell Jorner[a], Ferran Feixas[b], Rabia Ayub[a], Roland Lindh[c], Miquel Solà*[b] and Henrik Ottosson*[a]

Abstract: The low-lying triplet state of a recently published compound (**TMTQ**, *Angew. Chem. Int. Ed.* **2015**, *20*, 5888), was analyzed quantum chemically in light of suggestions that it is influenced by Baird-aromaticity. Two mesomeric structures describe this state; a zwitterionic Baird-aromatic structure with a triplet biradical 8π-electron methano[10]annulene (M10A) dicationic ring, and a Hückel-aromatic with a neutral closed-shell 10π-electron ring. According to charge and spin density distributions, the Hückel-aromatic structure dominates the triplet state (the Baird-aromatic contributes at most 12%), and separation of the FLU aromaticity index into α and β electron contributions emphasizes this finding. The small singlet-triplet energy gap is due to Hückel-aromaticity of the M10A ring, clarified by comparison to the smaller analogues of **TMTQ**. Yet, **TMTQ** and its analogues are Hückel-Baird hybrids allowing for tuning between closed-shell 4*n*+2 Hückel-aromaticity and open-shell 4*n* Baird-aromaticity.

Introduction

Aromaticity in the first ππ* excited triplet (T_1) state has recently received gradually increased attention.[1-3] Yet, the theoretical foundation was established in 1972 by Baird when he showed through perturbation molecular orbital theory that the π-electron counts for aromaticity and antiaromaticity of annulenes in their T_1 states are opposite to those given by Hückel's rule for the closed-shell singlet (ground) state (S_0).[4,5] Baird's rule, as it is now called,[1] has been confirmed by a range of different computational studies and it has also been suggested that it can be extended to electronic states of arbitrary spin.[6,7] Indeed, Baird's rule has been shown through computations to apply also to the first singlet excited state of cyclobutadiene, benzene and cyclooctatetraene,[8] and it could be a general back-of-an-envelope tool for the design of new optically and photochemically active molecules and functionalized materials.[5,9] Yet, its scope and limitations need to be resolved.

Recently, Tovar, Casado, and co-workers presented a compound (**TMTQ**, Figure 1) which exhibits a singlet-triplet energy gap (ΔE_{ST}) of only 4.9 kcal/mol (singlet more stable than triplet),[10] a fact that tentatively was attributed to stabilization of the T_1 state through Baird-aromaticity of the central 1,6-methano[10]annulene (M10A) fragment. In order for **TMTQ** to enjoy such T_1 state aromatic stabilization the mesomeric structure **TMTQ-c** with an 8π-electron 1,6-methano[10]annulenyl dication moiety ($M10A^{2+}$) must carry substantial weight. However, **TMTQ** in its T_1 state (^{3}**TMTQ**) can also be influenced by structure **TMTQ-b** with a closed-shell 10π-electron Hückel-aromatic ring and two terminal dicyanomethyl radicals. According to the DFT computations by Tovar, Casado and co-workers, the M10A fragment in ^{3}**TMTQ** displayed only small CC bond length alternation, clearly supporting aromatic character.[10] This interpretation was also confirmed by Raman spectroscopic data which revealed a more aromatic M10A core in T_1. Yet, the type of aromaticity, open-shell triplet Baird-aromaticity or closed-shell singlet Hückel-aromaticity, needs to be resolved.

Herein we address the electronic properties of **TMTQ** in its first triplet state, and also explore if this compound class can be further tailored with the aim to identify compounds that are more strongly Baird-aromatic in their T_1 states. As pointed out by Tovar, Casado and co-workers, these compounds could become important in π-conjugated spin-bearing materials,[10] and a correct understanding of their electronic structures should be of high importance. Our analysis is based on qualitative chemical bonding principles as well as on quantum chemical calculations.

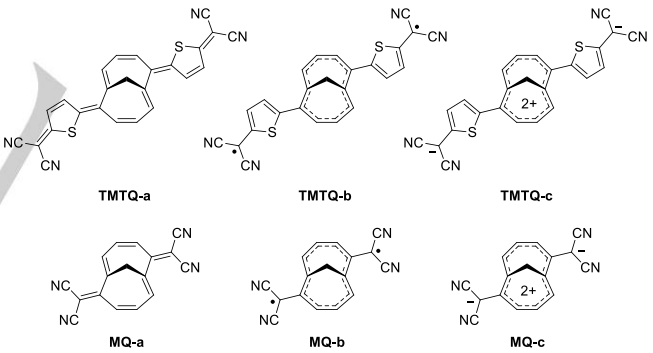

Figure 1. Covalent, diradical, and polar mesomeric structures of importance for compounds **TMTQ** and **MQ**.

Qualitative theory

At their highest possible symmetries, annulenyl (di)cations with 4*n* π-electrons are non-disjoint biradicals for which triplet ground states are expected from theory,[11] and they are also expected to be aromatic in their first triplet states according to Baird's rule. The most notable member of this compound class is the cyclopentadienyl cation, prepared by Saunders, Breslow, Wasserman and co-workers in 1973 and found by EPR spectroscopy to have a triplet ground state.[12] According to MRMP2 calculations, ΔE_{ST} = -11.9 kcal/mol at the D_{5h} geometry,[13] and in experiments, the triplet biradical was found to be below the

[a] M.Sc. Kjell Jorner, M.Phil. Rabia Ayub, Dr. Henrik Ottosson
Department of Chemistry – BMC
Uppsala University
Box 576, 75123 Uppsala, Sweden
E-mail: henrik.ottosson@kemi.uu.se
[b] Dr. Ferran Feixas, Prof. Dr. Miquel Solà
Institut de Química Computacional i Catàlisi (IQCC) and Departament de Química
Universitat de Girona
Campus de Montilivi s/n, 17071 Girona, Catalonia, Spain
Email: miquel.sola@udg.edu
[c] Prof. Dr. Roland Lindh
Department of Chemistry - Ångström Laboratory
Box 518, 75120 Uppsala, Sweden

Supporting information for this article, including computational details, ACID plots, NICS scans, atomic coordinates and analysis of Möbius aromaticity is given via a link at the end of the document.

most stable Jahn-Teller distorted singlet state structure by 4.4 kcal/mol,[14] in agreement with CCSDT calculations.[15] The aromaticity of the triplet cyclopentadienyl cation has also been confirmed by calculations of numerous aromaticity indices.[16] Indeed, a triplet biradical $4n$ π-electron cycle which is Baird-aromatic can be viewed as composed of a closed-shell Hückel-aromatic cycle with $4n$ - 2 π-electrons plus two non-bonding same-spin π-electrons (Figure 2a).[17] Alternatively, if the α- and β-spin π-electrons are regarded separately it can be viewed as composed of one Hückel-aromatic cycle with $2n$ + 1 π_α-electrons and one Hückel-aromatic cycle with $2m$ + 1 π_β-electrons where $n = m + 1$ (Figure 2b).[7,18] This last way to view Baird-aromatic cycles is useful when pinpointing the difference between Baird-aromatic and Hückel-aromatic cycles by computational means because the last type of cycles will have two equivalent π_α- and π_β-electron rings with equal values of various aromaticity indices while the first type of cycles will not.

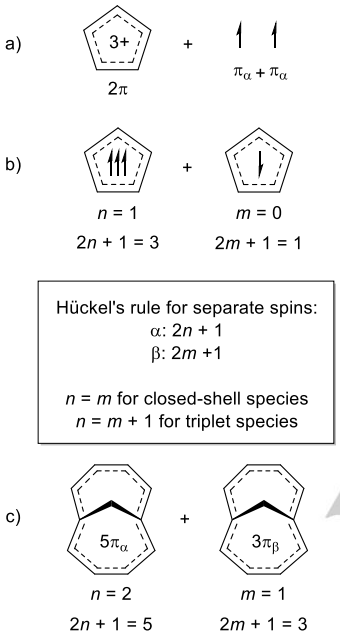

Figure 2. (a) Description of the cyclopentadienyl cation as a 2π-electron Hückel aromatic tricationic ring plus two non-bonding same-spin π electrons. (b, c) Analysis of the cyclopentadienyl cation and $M10A^{2+}$, showing them to be both α- and β-electron aromatic in their T_1 states according to Hückel's rule for separate spins.

The benzene dication $C_6H_6^{2+}$ at D_{6h} symmetry is also a non-disjoint biradical for which experiments have indicated a triplet ground state,[19] although CCSD(T) calculations place the singlet 2.2 kcal/mol below the triplet.[20] For the $C_{10}H_{10}^{2+}$ dication at D_{10h} symmetry, which is a fourth-order saddle point on the T_1 potential energy surface according to our calculations (see Supporting Information), full π-CI calculations within the Pariser-Parr-Pople model give ΔE_{ST} = -2.9 kcal/mol.[21] However, lowering of the symmetry to, *e.g.*, C_{2v} symmetry as in the M10A fragment, will stabilize the singlet state. In line with this reasoning, we now calculate ΔE_{ST} = -5.1 kcal/mol for the $C_{10}H_{10}^{2+}$ dication at D_{10h} symmetry with CASPT2,[22-25] while for the 1,6-methano[10]annulenyl dication (**$M10A^{2+}$**) we find ΔE_{ST} = 4.3 kcal/mol at the triplet Baird-aromatic C_{2v} geometry (see Supporting Information).

As noted above, **^{3}TMTQ** can be described as a zwitterion (**^{3}TMTQ-c**) with a $M10A^{2+}$ triplet Baird-aromatic 8π-electron ring ($5\pi_\alpha$ + $3\pi_\beta$).[10] Such a $M10A^{2+}$ ring should display the characteristics of an aromatic $5\pi_\alpha$-electron ring as well as the characteristics of an aromatic $3\pi_\beta$-electron ring (Figure 2c). Yet, it could also be described as a species (**^{3}TMTQ-b**) with a neutral closed-shell Hückel-aromatic M10A ring with ten π-electrons ($5\pi_\alpha$ + $5\pi_\beta$) which will have two equivalent 5π-electron rings (one $5\pi_\alpha$- and one $5\pi_\beta$-electron ring) with identical aromatic characteristics. As noted above, the separate consideration of aromatic α- and β-electron cycles will allow for the differentiation between a **TMTQ** molecule influenced primarily by **^{3}TMTQ-b** and one influenced primarily by **^{3}TMTQ-c**. Yet, it should be remarked that **^{3}TMTQ** and similar compounds in their triplet states have unique abilities to be simultaneously influenced by Hückel- and Baird-aromaticity, *i.e.*, it is a Hückel-Baird hybrid if both **^{3}TMTQ-b** and **^{3}TMTQ-c** contribute considerably to the electronic structure of the T_1 state. Still, for the labeling as a Baird-aromatic compound in its triplet state the mesomeric structure **^{3}TMTQ-c** must dominate the electronic structure. If instead **^{3}TMTQ-b** dominates, it is better labelled as a Hückel-aromatic compound influenced by Baird-aromaticity.

The change from a Hückel-aromatic to a Baird-aromatic species requires a change in electron count by two. Pentafulvenes are able to accomplish such a similar change because they are aromatic chameleons that can be influenced by a mesomeric structure with a Hückel-aromatic cyclopentadienyl anionic ring in the S_0 state and a Baird-aromatic cyclopentadienyl cationic ring in the T_1 state.[9,26-28] With proper substitution at the exocyclic and/or endocyclic positions the aromatic character can be enhanced in either the S_0 or the T_1 state, influencing the singlet-triplet energy gaps of substituted fulvenes.[26,28] Now the question is if two exocyclic dicyanomethylene moieties are capable to withdraw two electrons from the central M10A unit? In the second part of our study we investigated species with more strongly electron withdrawing aryl groups attached to the M10A unit. To what extent will these increase the influence of mesomeric structures such as **^{3}TMTQ-c**?

Results and Discussion

The purpose of the study reported herein was first to assess to what extent **TMTQ** is influenced by Baird-aromaticity in its T_1 state, and subsequently investigate one potential direction for how to increase this character. A series of different computational techniques were used in the assessment of the triplet state Baird-aromatic character. In the study by Tovar, Casado and co-workers, it was also proposed that **TMTQ** in the S_0 state (**^{1}TMTQ**) is influenced by Möbius aromaticity. In the Supporting Information we provide an analysis of this proposal and show this not to be the case.

Assessment of Baird-aromatic character from charge and spin densities

We now probed if **^{3}TMTQ** has a large influence of Baird-aromaticity and we first examined the charge and spin density distributions as these provide a first indication on the importance of mesomeric structure **^{3}TMTQ-c** as compared to **^{3}TMTQ-a** and **^{3}TMTQ-b**. Two conditions were applied in this analysis; (*i*) the triplet state should be described as an intramolecular charge-transfer state with a central M10A^{2+} ring, and (*ii*) sufficient spin density should be located on the M10A^{2+} fragment to justify it being described as a triplet biradical annulene. We consider that both conditions must be met simultaneously in order for **^{3}TMTQ** to be Baird aromatic.

To examine **TMTQ** against the first condition, we calculated atomic charges with B3LYP/6-311+G(d,p). [29,30] We also tested for the effect of DFT functional and basis set with OLYP[31] and M06-2X[32], as well as the B3LYP/6-31G(d,p) level[33] employed by Tovar, Casado, and co-workers[10] (see Supporting Information). As the results are similar, we report here only those from B3LYP/6-311+G(d,p). We summed the charges over the fragments of **^{3}TMTQ** (Table 1 and Tables SX). As atomic charges vary between methods, we calculated them with three different schemes: Natural Population Analysis (NPA),[34] Quantum Theory of Atoms-In-Molecules (QTAIM),[35] and CHELPG.[36] In addition, the Mulliken scheme[37] employed by Tovar and co-workers is included for comparison, although Mulliken charges are heavily basis set dependent[38] (also seen in Table SX). For the sake of brevity, we focus on the QTAIM results, which are very similar to those of CHELPG. While the NPA charges are in general smaller, the trends reported below are reproduced also for these. For the M10A unit, we give the percentage of the maximum +2 charge that would be present if **^{3}TMTQ-c** was totally dominant in parenthesis after the value of the charge.

The charge on the M10A fragment in **^{3}TMTQ** is +0.240 (12%) with QTAIM, which is even lower than the +0.286 (14%) in S_0. The corresponding negative QTAIM charge on the dicyanomethylene moieties in T_1 is -0.509, while the thiophene units carry +0.269. In S_0, the negative charge on the dicyanomethylene moieties is -0.577, while the thiophene units carry +0.291. Therefore, the calculations indicate that **TMTQ** is actually less polarized in T_1 than in S_0 and that **^{3}TMTQ-c** should have less weight.

However, these computational results are not consistent with the interpretation of experimental IR spectroscopic data given by Tovar, Casado and co-workers, who observed that the ũ(C≡N) wavenumber of **TMTQ** decreases by ~4 cm^{-1} upon heating.[10] Based on an established relationship between negative charge on the dicyanomethylene unit and ũ(C≡N) in TCNQ salts[39] (see also a more recent study[40]), it was suggested that this decrease corresponds to a greater shift of electron density towards the CN groups in the T_1 state, which is partially populated upon heating. Indeed, we obtain a calculated shift to lower wavenumbers of ca 30 cm^{-1} for ũ(C≡N) in **TMTQ** going from S_0 to T_1. However, it is not resolved if this shift is caused by radical delocalization into the dicyanomethylene groups (**TMTQ-b** dominant) or by charge delocalization to these moieties (**TMTQ-c** dominant). Calculations on model compounds in the Supporting Information suggest that both effects shift the ũ(C≡N) to lower wavenumbers. Therefore, one should also consider the alternative explanation that the shift ~~which is~~ observed is caused by influence of the diradical resonance structure **^{3}TMTQ-b**. *I.e.*, the interpretation of the IR spectroscopic data by Tovar, Casado and co-workers is not fully unambiguous.

These charge calculations therefore clarify that the weight of the dicationic resonance structure **TMTQ-c** in T_1 is less than in S_0, and at most 12%. With regard to the Mulliken charges they vary extensively with basis set and with method, with a difference of 0.899 e between the B3LYP/6-31G(d,p) and M06-2X/6-311+G(d,p) charges for the M10A unit in the S_0 state (Table SX).

Table 1. Charges and spin densities at the B3LYP/6-311+G(d,p) level for the M10A moiety of **^{1}TMTQ**, **^{3}TMTQ**, **^{1}MQ**, **^{3}MQ**, and **^{3}TMQ**. Values in parenthesis correspond to percentages of a charge of +2 and spin of 2.

	Charges				Spin densities		
	NPA	CHELPG	QTAIM	Mulliken	NPA	QTAIM	Mulliken
^{1}TMTQ	0.162 (8%)	0.370 (19%)	0.286 (14%)	0.909 (45%)	-	-	-
^{3}TMTQ	0.090 (4%)	0.250 (13%)	0.240 (12%)	0.687 (34%)	0.236 (12%)	0.257 (13%)	0.195 (10%)
^{1}MQ	0.494 (25%)	0.657 (33%)	0.551 (28%)	-	-	-	-
^{3}MQ	0.374 (19%)	0.480 (24%)	0.502 (25%)	-	0.653 (33%)	0.684 (34%)	0.614 (31%)
^{3}TMQ	0.251 (13%)	0.378 (19%)	0.370 (18%)	-	0.476 (24%)	0.498 (25%)	0.442 (22%)

Our second requirement for labeling **^{3}TMTQ** as Baird-aromatic is that sufficient spin density is localized on the M10A fragment. The plotted spin density (Figure 3a) indicates that only a minor part of the spin density is located on the M10A moiety, far from the appearance of the fully Baird-aromatic **^{3}M10A^{2+}** (Figure 3c). We carried out quantitative analysis based on the Mulliken, NPA, and QTAIM spin densities (Table 1), but as the results are very similar we discuss here only those from QTAIM. For **^{3}TMTQ**, only 13% is located on the M10A fragment, which is consistent with the charge value of 12%. In summary, the amount of Baird aromaticity, assessed based on the charge and spin density conditions, is limited by the charge and is thus at most 12%.

To assess the reliability of the DFT calculations, multi-reference RASPT2(28in28)/(4in4)/2 calculations[41] with the ANO-RCC-VTZP basis set[24] were carried out to probe if there is any effect of multi-configurational character for **TMTQ** either in S_0 or T_1 (for computational details, see the Supporting Information). For **^{1}TMTQ**, the closed-shell configuration is dominant with a weight of 0.65 while the second-most important has merely 0.04. Also for **^{3}TMTQ** one configuration dominates with 0.74 with the next one having 0.02.

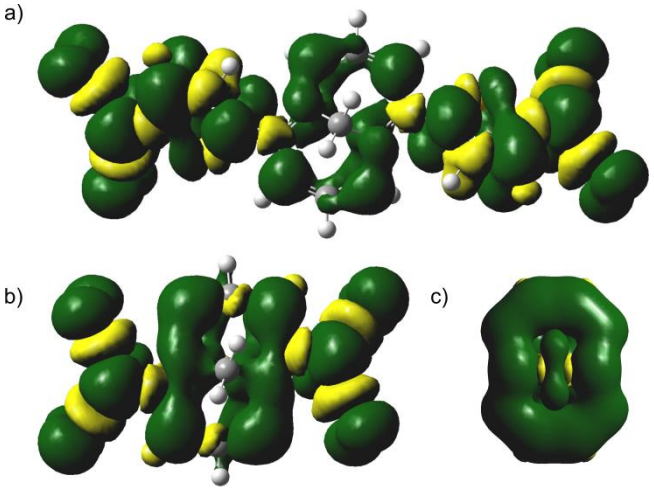

Figure 3. Spin densities at 0.0004 isosurface value for (a) **^{3}TMTQ**, (b) **^{3}MQ**, and (c) **^{3}M10A^{2+}**. Results with B3LYP/6-311+G(d,p).

These results show unambiguously that **TMTQ** in both S_0 and T_1 is well described by a single electronic configuration, and hence, there is good reason to believe that the DFT results are accurate. The RASSCF charges and spin densities are also consistent with those from DFT. For **^{3}TMTQ** the QTAIM charge on the M10A moiety is +0.238 (12%) with RASSCF, as compared to +0.240 (12%) with B3LYP, while the RASSCF Mulliken spin density is 0.141 (7%) as compared to 0.195 (10%) with B3LYP. For **^{1}TMTQ** the QTAIM charge on the M10A moiety is +0.295 (15%) with RASSCF, as compared to +0.286 (14%) with B3LYP. The results are also further confirmed with the LPNO-CEPA/1[42] and LPNO-CCSD[43] coupled cluster-type methods as calculated with ORCA[44] (see Supporting Information).

Assessment of Baird-aromatic character from aromaticity indices

We went on to study the aromaticity in the M10A fragment of **^{3}TMTQ** using aromaticity indices to determine (*i*) its extent of aromaticity, and (*ii*) whether it is primarily influenced by Hückel- or Baird-aromaticity. The results were compared to 1,6-methano[10]annulene in S_0 (**^{1}M10A**, 10 π-electrons, Hückel-aromatic) and **M10A^{2+}** in T_1 (**^{3}M10A^{2+}**, 8 π-electrons, Baird-aromatic). Results are given for B3LYP/6-311+G(d,p). According to HOMA,[45] **^{3}TMTQ** is clearly aromatic (0.836) but it is unclear if it is more similar to **^{1}M10A** (0.887) or to **^{3}M10A^{2+}** (0.761). The ACID[46] plot (Figure 4) and the NICS scan[47] (Figure 5) further confirm that **^{3}TMTQ** is aromatic, although comparison with **^{1}M10A** (Figures S21-22) and **^{3}M10A^{2+}** (Figures S23-24) does not readily reveal whether it is Hückel- or Baird-aromatic. We further calculated the electronic aromaticity index FLU (see Table S6).[48] A FLU value of 0.005 again indicates that **^{3}TMTQ** is aromatic (low FLU values are found for aromatic species), a value which is similar to 0.004 for **^{1}M10A** and 0.006 for **^{3}M10A^{2+}**. In contrast, a FLU value of 0.025 for **^{1}TMTQ** indicates non-aromaticity, which is further confirmed by the ACID plot (Figure S8), NICS scan (Figure S7), and HOMA value (0.279). The calculated multicenter indices (MCI)[49] for the M10A moiety of 0.001 for **^{1}TMTQ** and of 0.006 for **^{3}TMTQ**, as compared to 0.009 for **^{1}M10A** and 0.011 for **^{3}M10A^{2+}**, are also in line with **TMTQ** being non-aromatic in S_0 and aromatic in T_1, respectively.

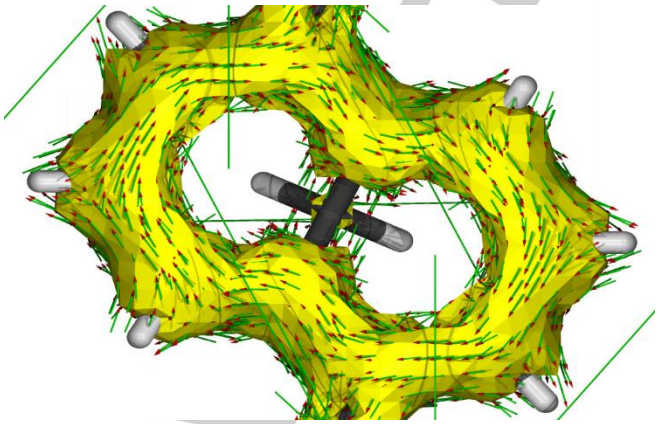

Figure 4. ACID plot of the M10A moiety of **^{3}TMTQ**. Isosurface value at 0.050 a.u. Clockwise current indicates aromaticity. Results with CSGT-B3LYP/6-311+G(d,p).

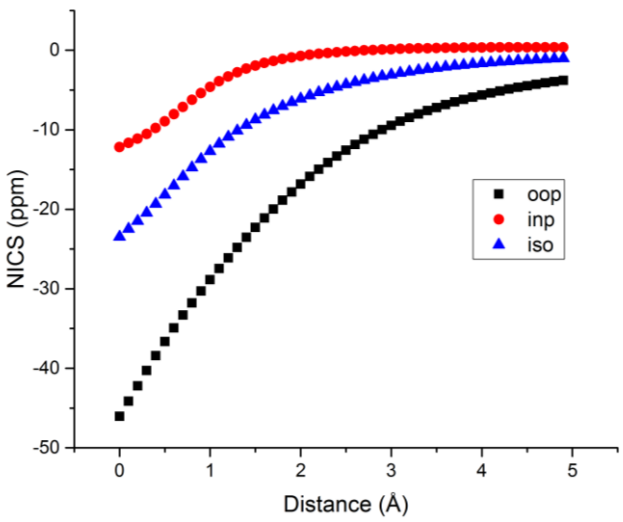

Figure 5. NICS scan for the M10A moiety of **^{3}TMTQ**. A deep minimum for the out-of-plane component indicates aromaticity. Results with GIAO-B3LYP/6-311+G(d,p).

Yet, the question is whether **^{3}TMTQ** is Hückel- or Baird-aromatic? To answer this question we dissected the FLU values into separate contributions from the α and β electrons. Based on what is described above, we expect to find identical or very similar values of FLU_α and FLU_β in Hückel-aromatic species and significant differences ($\Delta FLU_{\alpha\beta} = FLU_\alpha - FLU_\beta \neq 0$) in Baird-aromatic systems ~~(see Figure 3c)~~. This strategy has previously been used for multicenter delocalization indices and NICS values

to analyze aromaticity in open-shell annulenes.[18] To make consistent comparisons between species with different absolute aromaticity, it is possible to use the $\Delta FLU_{\alpha\beta}/FLU$ ratio. Our results (Table 3) reveal that for **^{3}M10A^{2+}**, which is Baird-aromatic, the $\Delta FLU_{\alpha\beta}/FLU$ value was as large as -2.000. On the contrary, $\Delta FLU_{\alpha\beta}/FLU$ is only -0.223 for the M10A ring of **^{3}TMTQ**, which clearly supports the Hückel-aromatic character of this ring.

Table 2. FLU, FLU_α, FLU_β, $\Delta FLU_{\alpha\beta}$, and $\Delta FLU_{\alpha\beta}/FLU$ values for **^{3}TMTQ**, **^{3}MQ**, **^{3}TMQ** and **^{3}M10A^{2+}** in T_1 at the B3LYP/6-311+G(d,p) level.

	^{3}TMTQ	**^{3}MQ**	**^{3}TMQ**	**^{3}M10A^{2+}**
FLU	0.0046	0.0068	0.0063	0.0058
FLU_α	0.0041	0.0044	0.0045	0.0029
FLU_β	0.0052	0.0106	0.0091	0.0145
$\Delta FLU_{\alpha\beta}$	-0.00110	-0.0062	-0.0046	-0.0116
$\Delta FLU_{\alpha\beta}/FLU$	-0.2233	-0.9113	-0.7337	-2.0005

We also assessed the change in aromaticity of the thiophene rings when going from the S_0 state to the T_1 state. Both HOMA (from 0.438 to 0.743), FLU (from 0.018 to 0.005), and MCI (from 0.012 to 0.020) indicate that the aromaticity increases when going from S_0 to T_1. Taken together, the results are consistent with a description of **^{1}TMTQ** primarily by the quinoidal resonance structure **^{1}TMTQ-a** with minor inclusion of **^{1}TMTQ-c**, while **^{3}TMTQ** is described primarily by **^{3}TMTQ-b** with slight inclusion of **^{3}TMTQ-c**.

Effect of charge and spin delocalization

Hence, our results reveal that **^{3}TMTQ** has only little influence of Baird-aromaticity. However, compound **MQ** (Figure 1), which unfortunately could not be synthesized by Tovar, Casado and co-workers,[10] will have a lower tendency to delocalize spin and charge away from the M10A fragment, and should therefore have a greater influence of Baird aromaticity. Results with B3LYP/6-311+G(d,p) (Table 1) shows that the QTAIM charge of the M10A fragment is +0.502 (25%) for **^{3}MQ** which is more than twice than the +0.240 (12%) of **^{3}TMTQ**. As for spin density, 34% is on the M10A fragment in **^{3}MQ** as compared to 13% in **^{3}TMTQ** (Figure 3b, Table 1). The amount of Baird aromaticity is thus limited by the charge condition (as given above) and is at most 25%. These results are also consistent with those from RASSCF(20in20)/(4in4)/2, LPNO-CEPA/1 and LPNO-CCSD (see Supporting Information). The HOMA value of **^{3}MQ** (0.781) is smaller than for **^{3}TMTQ** (0.836), and closer to that of **^{3}M10A^{2+}** (0.761) than **^{1}M10A** (0.887). The ACID plot and NICS scan further support its aromatic character (Figures S13-14). Both MCI of 0.004 and FLU of 0.007 for **^{3}MQ** are in agreement with previous descriptors. Interestingly, $\Delta FLU_{\alpha\beta}/FLU$ of -0.911 for the M10A ring of **^{3}MQ** indicates aromatic character intermediate between that of a Hückel and a Baird species, clearly showing that the compound class can be described as Hückel-Baird hybrids in their triplet states. In contrast, **^{1}MQ** is non-aromatic according to HOMA (0.124), ACID (Figure S12), NICS scan (Figure S11), MCI (0.001), and FLU (0.032). In conclusion, **MQ** is a promising candidate for a more Baird aromatic compound, yet, its ΔE_{ST} is 18.5 kcal/mol with B3LYP/6-311+G(d,p) as compared to 5.0 kcal/mol for **TMTQ**.

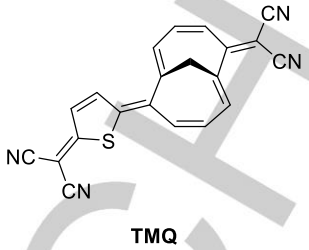

TMQ

Figure 6. Structure of **TMQ**.

Cause for low ΔE_{ST}

So what is the cause for the low ΔE_{ST} of **TMTQ** if it is not primarily Baird aromaticity? To answer this question we also calculated **TMQ** (Figure 6), having only one thiopheno ring. The M10A moiety of this compound in its T_1 state has a QTAIM charge of +0.370 (18%), a spin density of 25% (Table 1), and the compound has a ΔE_{ST} of 10.8 kcal/mol. These are all values which lie in between those of **TMTQ** and **MQ**. The ACID plot and NICS scan show that it is aromatic in T_1 (Figure SY and SX), and this is also supported by a HOMA value of 0.786 and FLU value of 0.006. The $\Delta FLU_{\alpha\beta}/FLU$ is -0.733 for the M10A ring of **^{3}TMQ**, which also indicate a higher Baird-aromatic character than **^{3}TMTQ** (see Table 2).

Thus, for the series of **MQ**, **TMQ** and **TMTQ** we find ΔE_{ST} values of 18.5, 10.8 and 5.0 kcal/mol at the B3LYP/6-311+G(d,p) level, and the low ΔE_{ST} of **TMTQ** is primarily due to the presence of several pro-aromatic units rather than a Baird-aromatic dicationic M10A moiety. **MQ** has the highest Baird aromaticity, and at the same time the highest ΔE_{ST}. However, Tovar, Casado and co-workers argue that the ΔE_{ST} of **TMTQ** is remarkably low compared to other compounds of similar size. If this was the case, it would fit with a different type of stabilization, such as due to Baird aromaticity. Tovar, Casado and co-workers point out that **Q3TCN**, with three pro-aromatic thiophene moieties, displays a calculated ΔE_{ST} of 6.9 kcal/mol, compared to 4.4 kcal/mol for **TMTQ** while we have to go to **Q4TCN** with four thiophene moieties to get to 4.1 kcal/mol.[50] However, we note that a compound with three pro-aromatic *p*-quinodimethane units and a ΔE_{ST} of 2.1 kcal/mol, even lower than **TMTQ**, has been reported.[51] As **TMTQ** has a ΔE_{ST} in line with previously reported compounds of similar size, there is no need to invoke Baird aromaticity to account for this value.

A test on the enhancement of Baird-aromatic character

So is it possible to enhance the Baird-aromatic character of the central M10A unit by increasing the electron-withdrawing strength of the aryl substituents? To answer this question, we investigated **TMTQ** and **TMQ** with fluoro and cyano substituents on the thiopheno rings as well as the corresponding compounds where the thiopheno moieties are replaced by substituted *p*-quinodimethane units (Figure 7).

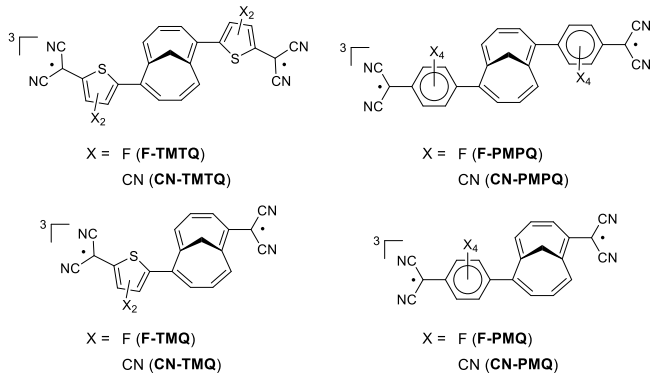

Figure 7. Structures of **X-TMTQ**, **X-PMPQ**, **X-TMQ**, and **X-PMQ**.

Here we focus the analysis on (*i*) the difference between thiopheno and *p*-quinodimethane units, and (*ii*) the difference between CN and F as the former is mainly π-withdrawing while the latter is σ-withdrawing. Our results with B3LYP/6-311+G(d,p) and QTAIM show that the charge polarization (measured as percentage of the maximum +2 charge on the M10A unit) is increased by going from **^{3}TMTQ** (12%) to either **^{3}CN-TMTQ** (21%) or **^{3}F-TMTQ** (18%). However, this is accompanied by a small decrease in spin density from 13% to 9% and 12%, respectively, which overall leads to no major change in Baird aromaticity. The withdrawal of spin density is even larger in **^{3}CN-PMPQ** (2%) and **^{3}F-PMPQ** (6%), showing that a switch from thiopheno to *p*-quinodimethane is not a viable strategy to increase the Baird aromaticity of **^{3}TMTQ**. However, with only one thiopheno or *p*-quinodimethane unit, spin density is retained better, with **^{3}F-TMQ** (25%), **^{3}CN-TMQ** (24%), **^{3}F-PMQ** (23%) and **^{3}CN-PMQ** (22%) being comparable to **^{3}TMQ** (25%). At the same time the charge polarization for **^{3}F-TMQ** (21%), **^{3}CN-TMQ** (23%), **^{3}F-PMQ** (21%), and **^{3}CN-PMQ** (22%) is slightly higher than in **^{3}TMQ** (18%). All these observations are also supported by $\Delta FLU_{\alpha\beta}$, and $\Delta FLU_{\alpha\beta}$/FLU measures (see Table SX) showing that high $\Delta FLU_{\alpha\beta}$/FLU values are obtained for **^{3}F-TMQ** (-0.662), **^{3}CN-TMQ** (-0.621), **^{3}F-PMQ** (-0.697), and **^{3}CN-PMQ** (-0.626), while low ones are obtained for **^{3}F-TMTQ** (-0.222), **^{3}CN-TMTQ** (-0.195), **^{3}F-PMPQ** (-0.093), and **^{3}CN-PMPQ** (-0.022). Overall, the smaller compounds display a modest effect from the EWGs that increase the Baird aromatic character slightly. There is no significant difference between thiopheno or *p*-quinodimethane, or between fluoro or cyano substituents as EWGs in this case.

Conclusions

In summary, the study of Tovar, Casado, and co-workers points to a new and interesting class of compounds which in their T_1 states are influenced both by Hückel and Baird aromaticity in the same ring. Although the influence of Baird aromaticity in **^{3}TMTQ** is limited to ~12% at most, the influence in the related **^{3}MQ** is the double (maximum ~25%). Adding electron-withdrawing groups on the thiopheno moieties of **TMTQ** and **TMQ** and exchanging for *p*-quinodimethane units as in **PMQ** and **PMPQ** lead to compounds with similar or even smaller Baird aromatic character. It should be noted that Tovar, Casado and co-workers also found a low singlet excitation energy for **TMTQ** which they tentatively attributed to stabilization of the S_1 state due to Baird aromaticity.[10] Considering a potentially larger charge-transfer character in S_1 as compared to T_1, this may well be the situation. Yet, this hypothesis needs a separate computational investigation.

Finally, we note that Baird's rule should be an elegant and general back-of-an-envelope tool for design of a range of functionalized molecules and materials with targeted electronic and optical properties,[5,9] including compounds for use in π-conjugated spin-bearing materials.[10] The field of excited state aromaticity and antiaromaticity truly represents a new vista for physical organic chemistry which, however, requires a close interaction between experiments and theory for the most efficient progress and development as a correct understanding of the electronic structure is crucial.

Acknowledgements

We would first like to thank Profs. J. D. Tovar and J. Casado for fruitful discussions on the compounds examined herein. This work has been supported by the Swedish Research Council (project grant 621-2011-4177), Ministerio de Economía y Competitividad (MINECO) of Spain (Project CTQ2014-54306-P) and the Generalitat de Catalunya (project 2014SGR931, Xarxa de Referència en Química Teòrica i Computacional, and ICREA Academia 2014 prize for M.S.). F.F. acknowledges financial support of the Beatriu de Pinós programme from AGAUR for the postdoctoral grants BP_A_00339 and BP_A2_00022. M.S. and F.F. are grateful to the European Union (EU) for FEDER fund number UNGI10-4E-801. The Swedish National Infrastructure for Computation (SNIC) through NSC, Linköping, is acknowledged for computer time. We are grateful to Prof. R. Herges and Prof. A. Stanger for providing the AICD and Aroma programs, respectively.

Computational methods

All quantum-chemical calculations were done using Gaussian09, revision D.01,[52] Molcas 8.1,[23] and ORCA 3.0.3,[44] The structure of **TMTQ** was optimized separately with the OLYP,[31] B3LYP,[29] and M06-2X[32] functionals with the 6-311+G(d,p) basis set,[30] as well as the B3LYP/6-31G(d,p) level.[33] For the rest of the molecules in the study, B3LYP/6-311+G(d,p) was used unless otherwise noted. Cartesian coordinates and energies of all compounds considered are found in the Supporting Information. CASSCF,[53] RASSCF,[54] CASPT2,[22] and RASPT2[41] calculations employed the ANO-RCC basis sets[24] using the B3LYP/6-311+G(d,p) geometries. LPNO-CEPA/1[42] and LPNO-CCSD[43] calculations employed the cc-pVTZ basis set[55] on the B3LYP/6-311+G(d,p) geometries. Details on these calculations are given in the Supporting Information. Some calculations also employed the CCSD(T) method[56] and the CAM-B3LYP[57]functional. Atomic charges have been calculated using the Natural Population Analysis (NPA),[34] Quantum Theory of Atoms-In-Molecules (QTAIM),[35] and CHELPG[36] schemes, in addition to the Mulliken charges.[37] NBO 6.0,[58] and Multiwfn 3.3.7[59] were used for NPA and QTAIM charge analysis, respectively, while Gaussian09 was used for Mulliken and CHELPG charges. QTAIM analysis was done using the "medium quality grid" with a spacing of 0.1 Bohr. The integration of charge and spin density in the QTAIM basis was done using mixed grids, with exact refinement of the

basis boundaries (option 7, 2 in Multiwfn). Spin densities were calculated using the Mulliken, QTAIM and NPA schemes in an analogous way to the charges.

ACID[46] plots are a general method to visualize conjugation and ring currents. Ring current maps have previously been used to analyze triplet state aromaticity, although with another method.[60] Clockwise currents indicate aromaticity, while weak and/or chaotic currents indicate non-aromaticity. ACID plots were generated with the AICD 2.0.0 program at the CSGT-B3LYP/6-311+G(d,p) level of theory[46] at 0.050 a.u. isosurface. The NICS scan[47] method can be used to assess the magnetic aspect of aromaticity. Deep minima for the out-of-plane component are indicative of aromaticity, while shallow minima are indicative of non-aromaticity. The NICS scans were generated with the Aroma 1.0 package[47] at the GIAO-B3LYP/6-311+G(d,p)[61] level of theory. The coordinates for the bq atoms of the NICS scan are given at the end of the Supporting Information together with the coordinates for the respective compound.

The harmonic oscillator model of aromaticity (HOMA)[45] measures the geometric aspect of aromaticity and was calculated with Multiwfn 3.3.7.[59] Values close to 1 correspond to aromaticicity and values close to 0 to non-aromaticity. The aromatic fluctuation index (FLU)[48] and multicenter index (MCI)[49] measure the electronic aspect of aromaticity. Lower values correspond to higher aromaticity for FLU, while higher values correspond to higher aromaticity for MCI. Calculations of FLU and MCI were performed with the AIMPAC[62] and ESI-3D[63] collection of programs. Further details of the MCI and FLU calculations are found in the Supporting Information.

Keywords: annulenes • aromaticity • Baird's rule • biradical species • electronic structure

[1] M. Rosenberg, C. Dahlstrand, K. Kilså, H. Ottosson, *Chem. Rev.* **2014**, *114*, 5379-5425
[2] R. Papadakis, H. Ottosson, *Chem. Soc. Rev.* **2015**, *44*, 6472-6493.
[3] Y. M. Sung, M.-C. Yoon, J. M. Lim, H. Rath, K. Naoda, A. Osuka, D. Kim, *Nat. Chem.* **2015**, 7, 418-422.
[4] N. C. Baird, *J. Am. Chem. Soc.* **1972**, 94, 4941-4948.
[5] H. Ottosson, *Nat. Chem.* **2012**, 4, 969-971.
[6] A. Soncini, P. W. Fowler, *Chem. Phys. Lett.* **2008**, 450, 431-436.
[7] A. Soncini, P. W. Fowler, *Chem. - Eur. J.* **2013**, 19, 1740-1746.
[8] (a) M. Kataoka, *J. Chem. Res.* **2004**, *2004*, 573-574. (b) P. B. Karadakov, *J. Phys. Chem. A* **2008**, 112, 7303-7309. (c) P. B. Karadakov, *J. Phys. Chem. A* **2008**, 112, 12707-12713. (d) F. Feixas, J. Vandenbussche, P. Bultinck, E. Matito, M. Solà, *Phys. Chem. Chem. Phys.* **2011**, 13, 20690-20703.
[9] H. Möllerstedt, M. C. Piqueras, R. Crespo, H. Ottosson, *J. Am. Chem. Soc.* **2004**, 126, 13938-13939.
[10] B. C. Streifel, J. L. Zafra, G. L. Espejo, C. J. Gómez-García, J. Casado, J. D. Tovar, *Angew. Chem., Int. Ed.* **2015**, *54*, 5888–5893; *Angew. Chem.* **2015**, *127*, 5986–5991.
[11] (a) W. T. Borden, E. R. Davidson, *J. Am. Chem. Soc.* **1977**, *99*, 4587-4594; (b) W. T. Borden, H. Iwamura, J. A. Berson, *Acc. Chem. Res.* **1994**, *27*, 109-116.
[12] M. Saunders, R. Berger, A. Jaffe, J. M. McBride, J. O'Neill, R. Breslow, J. M. Hoffmann, C. Perchonock, E. Wasserman, R. S. Hutton, V. J. Kuck, *J. Am. Chem. Soc.* **1973**, *95*, 3017-3018.
[13] D. W. Small, E. J. Sundstrom, M. Head-Gordon, *J. Chem. Phys.* **2015**, *142*, 024104.
[14] (a) H. J. Wörner, F. Merkt, *J. Chem. Phys.* **2007**, *127*, 034303; (b) H. J. Wörner, F. Merkt, *Angew. Chem., Int. Ed.* **2009**, *48*, 6404-6424; *Angew. Chem.* **2009**, *121*, 6524–6545.
[15] P.-K. Lo, K.-C. Lau, *J. Phys. Chem. A* **2014**, *118*, 2498-2507.
[16] V. Gogonea, P. v. R. Schleyer, P. R. Schreiner, *Angew. Chem., Int. Ed.* **1998**, *37*, 1945-1948; *Angew. Chem.* **1998**, 110, 2045–2049.
[17] S. Zilberg, Y. Haas, *J. Phys. Chem. A* **1998**, *102*, 10851-10859.
[18] M. Mandado, A. M. Graña, I. Pérez-Juste, *J. Chem. Phys.* **2008**, *129*, 164114-164114.
[19] J. H. D. Eland, *Chem. Phys.* **2008**, *345*, 82-86.
[20] R. Marzio, C. W. Bauschlicher, Jr., E. L. O. Bakes, *Astrophys. J.* **2004**, *609*, 1192.
[21] S. Kuwajima, Z. G. Soos, *J. Am. Chem. Soc.* **1987**, *109*, 107-113.
[22] K. Andersson, P.-Å. Malmqvist, B. O. Roos, *J. Chem. Phys.* **1992**, *96*, 1218-1226.
[23] Aquilante, F. et. al., *J. Comput. Chem.* **2015**, DOI: 10.1002/jcc.24221. For full reference, see Supporting Information.
[24] B. O. Roos, R. Lindh, P.-Å. Malmqvist, V. Veryazov, P.-O. Widmark, *J. Phys. Chem. A* **2003**, *108*, 2851-2858.
[25] Calculations with Molcas 8.0 (ref. 23) and the ANO-RCC-VTZP basis set (ref. 24) using an active space of 8 electrons in 10 orbitals.
[26] H. Ottosson, K. Kilså, K. Chajara, M. Piqueras, R. Crespo, H. Kato, D. Muthas, *Chem. - Eur. J.* **2007**, *13*, 6998-7005
[27] Dahlstrand, C., Rosenberg, M. Kilså, K., Ottosson, H. *J. Phys. Chem. A* **2012**, *116*, 5008-5017
[28] K. Jorner, R. Emanuelsson, C. Dahlstrand, H. Tong, A. V. Denisova, H. Ottosson, *Chem. - Eur. J.* **2014**, *20*, 9295-9303.
[29] P. J. Stephens, F. J. Devlin, C. F. Chabalowski, M. J. Frisch, *J. Phys. Chem.* **1994**, *98*, 11623-11627.
[30] R. Krishnan, J. S. Binkley, R. Seeger, J. A. Pople, *J. Chem. Phys.* **1980**, *72*, 650-654.
[31] N. C. Handy, A. J. Cohen, *Mol. Phys.* **2001**, *99*, 403-412.
[32] Y. Zhao, D. Truhlar, *Theor. Chem. Acc.* **2008**, *120*, 215-241.
[33] W. J. Hehre, R. Ditchfield, J. A. Pople, *J. Chem. Phys.* **1972**, *56*, 2257-2261.
[34] A. E. Reed, R. B. Weinstock, F. Weinhold, *J. Chem. Phys.* **1985**, *83*, 735-746.
[35] R. F. W. Bader, *Chem. Rev.* **1991**, *91*, 893-928.
[36] C. M. Breneman, K. B. Wiberg, *J. Comput. Chem.* **1990**, *11*, 361-373.
[37] R. S. Mulliken, *J. Chem. Phys.* **1955**, *23*, 1833-1840.
[38] C. J. Cramer, *Essentials of computational chemistry: theories and models*, 2nd ed., Wiley, Chichester, U. K., **2004**.
[39] J. S. Chappell, A. N. Bloch, W. A. Bryden, M. Maxfield, T. O. Poehler, D. O. Cowan, *J. Am. Chem. Soc.* **1981**, 103, 2442-2443.
[40] T. Mani, D. C. Grills, M. D. Newton, J. R. Miller, *J. Am. Chem. Soc.* **2015**, *137*, 10979-10991.
[41] P. Å. Malmqvist, K. Pierloot, A. R. M. Shahi, C. J. Cramer, L. Gagliardi, *J. Chem. Phys.* **2008**, 128, 204109.
[42] F. Neese, F. Wennmohs, A. Hansen, *J. Chem. Phys.* **2009**, 130, 114108.
[43] F. Neese, A. Hansen, D. G. Liakos, *J. Chem. Phys.* **2009**, 131, 064103.
[44] F. Neese, *Wiley Interdiscip. Rev.: Comput. Mol. Sci.* **2012**, 2, 73-78.
[45] (a) J. Kruszewski, T. M. Krygowski, *Tetrahedron Lett.* **1972**, *13*, 3839-3842; (b) T. M. Krygowski, *J. Chem. Inf. Comput. Sci.* **1993**, *33*, 70-78.
[46] (a) R. Herges, D. Geuenich, *J. Phys. Chem. A* **2001**, *105*, 3214-3220; (b) D. Geuenich, K. Hess, F. Kohler, R. Herges, *Chem. Rev.* **2005**, *105*, 3758-3772; (c) Calculations carried out with the AICD 2.0.0 program kindly provided by Rainer Herges.
[47] (a) A. Stanger, *J. Org. Chem.* **2006**, *71*, 883-893; (b) J. O. C. Jiménez-Halla, E. Matito, J. Robles, M. Solà, *J. Organomet. Chem.* **2006**, *691*, 4359-4366; (c) NICS scans performed with the Aroma 1.0 package: A. Rahalkar, A. Stanger, "Aroma", http://schulich.technion.ac.il/Amnon_Stanger.htm.
[48] (a) E. Matito, M. Duran, M. Solà, *J. Chem. Phys.* **2005**, *122*, 014109; (b) Erratum: E. Matito, M. Duran, M. Solà, *J. Chem. Phys.* **2006**, *125*, 059901; (c) F. Feixas, E. Matito, J. Poater, M. Solà, *Chem. Soc. Rev.* **2015**, *44*, 6434-6451.

[49] P. Bultinck, R. Ponec, S. Van Damme, *J. Phys. Org. Chem.* **2005**, *18*, 706-718.

[50] R. Ponce Ortiz, J. Casado, V. Hernández, J. T. López Navarrete, E. Ortí, P. M. Viruela, B. Milián, S. Hotta, G. Zotti, S. Zecchin, B. Vercelli, *Adv. Funct. Mater.* **2006**, 16, 531-536.

[51] X. Zhu, H. Tsuji, K. Nakabayashi, S.-i. Ohkoshi, E. Nakamura, *J. Am. Chem. Soc.* **2011**, 133, 16342-16345.

[52] Gaussian09, Revision D.01, M. J. Frisch et al., Gaussian, Inc., Wallingford, CT, USA, **2009**. Full reference given in the Supporting Information.

[53] B. O. Roos, P. R. Taylor, P. E. M. Siegbahn, *Chem. Phys.* **1980**, 48, 157-173.

[54] J. Olsen, B. O. Roos, P. Jørgensen, H. J. A. Jensen, *J. Chem. Phys.* **1988**, 89, 2185-2192.

[55] (a) T. H. Dunning, *J. Chem. Phys.* **1989**, 90, 1007-1023. (b) D. E. Woon, T. H. Dunning, *J. Chem. Phys.* **1993**, 98, 1358-1371.

[56] K. Raghavachari, G. W. Trucks, J. A. Pople, M. Head-Gordon, *Chem. Phys. Lett.* **1989**, 157, 479-483.

[57] T. Yanai, D. P. Tew, N. C. Handy, *Chem. Phys. Lett.* **2004**, 393, 51-57.

[58] NBO 6.0, E. D. Glendening, K. B. J, A. E. Reed, J. E. Carpenter, J. A. Bohmann, C. M. Morales, C. R. Landis, F. Weinhold, Theoretical Chemistry Institute, University of Wisconsin, Madison, **2013**.

[59] T. Lu, F. W. Chen, *J. Comput. Chem.* **2012**, *33*, 580-592.

[60] P. W. Fowler, E. Steiner, L. W. Jenneskens, *Chem. Phys. Lett.* **2003**, 371, 719-723.

[61] K. Wolinski, J. F. Hinton, P. Pulay, *J. Am. Chem. Soc.* **1990**, 112, 8251-8260.

[62] F. W. Biegler-König, R. F. W. Bader, T.-H. Tang, *J. Comput. Chem.* **1982**, 3, 317-328. (http://www.chemistry.mcmaster.ca/aimpac/)

[63] E. Matito, ESI-3D: Electron Sharing Indexes Program for 3D Molecular Space Partitioning. http://iqc.udg.edu/~eduard/ESI, Institute of Computational Chemistry: Girona, 2006.

Entry for the Table of Contents (Please choose one layout)

Layout 1:

FULL PAPER

Smoothly opening the closed shell by mixing closed-shell Hückel-aromaticity with open-shell Baird-aromaticity; this is possible in the first triplet states of recently published compounds which can be described as triplet biradical Hückel-Baird aromatic hybrids (see Figure). Yet, our quantum chemical analysis shows that the triplet state aromatic hybrids that hitherto have been presented are primarily Hückel-aromatic, pointing to directions for future molecular design.

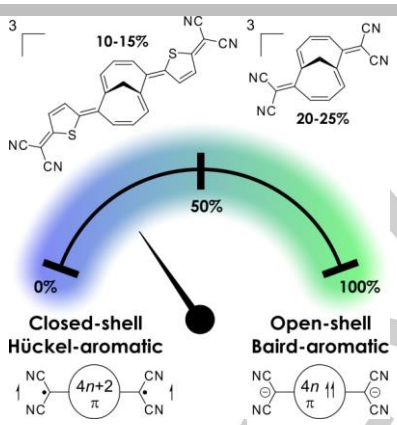

Kjell Jorner, Ferran Feixas, Rabia Ayub, Roland Lindh, Miquel Solà and Henrik Ottosson**

Page No. – Page No.

Analysis of a Compound Class with Triplet States Stabilized by Potentially Baird-Aromatic [10]Annulenyl Dicationic Rings